PHYSICAL REVIEW C **93**, 031902(R) (2016)

Femto-vortex sheets and hyperon polarization in heavy-ion collisions

Mircea Baznat,[1,2,*] Konstantin Gudima,[1,2,†] Alexander Sorin,[1,3,‡] and Oleg Teryaev[1,3,§]

[1]*Joint Institute for Nuclear Research, 141980 Dubna (Moscow Region), Russia*

[2]*Institute of Applied Physics, Academy of Sciences of Moldova, MD-2028 Kishinev, Moldova*

[3]*National Research Nuclear University MEPhI (Moscow Engineering Physics Institute), Kashirskoe Shosse 31, 115409 Moscow, Russia*

(Received 7 October 2015; revised manuscript received 20 January 2016; published 4 March 2016)

We study the structure of vorticity and hydrodynamic helicity fields in peripheral heavy-ion collisions using the kinetic quark-gluon string model. The angular momentum conservation within this model holds with a good accuracy. We observe the formation of specific toroidal structures of vorticity field (vortex sheets). Their existence is mirrored in the polarization of hyperons of the percent order.

DOI: 10.1103/PhysRevC.93.031902

Introduction. The local violation [1] of discrete symmetries in strongly interacting QCD matter is now under intensive theoretical and experimental investigations. The renowned chiral magnetic effect (CME) uses the $(C)P$-violating (electro)magnetic field that emerges in heavy-ion collisions in order to probe the $(C)P$-odd effects in QCD matter.

There is an interesting counterpart of this effect, chiral vortical effect (CVE) [2], due to the coupling to P-odd medium vorticity leading to the induced electromagnetic as well as all conserved-charge currents [3], in particular the baryonic one.

Another important P-odd observable is the baryon polarization. The mechanism analogous to CVE (known as axial vortical effect, see Ref. [4] and references therein) leads to induced axial current of strange quarks. This current may be converted to polarization of Λ hyperons [3,5,6]. Another mechanism of this polarization is provided by so-called thermal vorticity in the hydrodynamical approach [7].

The zeroth component of axial current and the corresponding axial charge are related to hydrodynamical helicity

$$H \equiv \int dV(\vec{v}\cdot\vec{w}),$$

which is the projection of velocity $\vec{v}$ to vorticity $\vec{w} = curl\vec{v}$. This quantity manifests the recently discovered [5] and confirmed [8] phenomenon of the separation, i.e., its mirror behavior with the same magnitudes but with different signs in the half-spaces separated by the reaction plane. This mirror behavior may be naturally explained [5] by the contribution of y component of vorticity. This contribution is not only the single one in the hydrodynamical approach [7,9–11] but also essential (however, accompanied by the longitudinal component of the same order [5]) in the kinetic model.

The noncentral heavy-ion collisions could naturally generate a rotation (global or local, both related to vorticity) with an angular velocity normal to the reaction plane, which is their generic qualitative feature. Though it is natural to expect that the angular momentum conservation plays an essential role in defining the quantitative properties of vortical effects, it remains to be studied to which extent the particles, carrying the main part of angular momentum, participate in the collisions.

In this work, we address these problems by performing extensive numerical simulations. We explore the distribution of angular momentum and find that the role of participating nucleons is relatively small, albeit noticeable. We study, in some detail, the structure of vorticity field and apply it to different approaches to polarization calculations. We observed that the peculiar toroidal tirelike structure manifests itself in the polarization of hyperons. We find that different approaches to polarization calculations lead to qualitatively similar results.

Angular momentum conservation in the kinetic model. The natural source of the P-odd observables in heavy-ion collisions is the pseudovector of angular momentum. The question that immediately emerges is whether it is conserved in the course of evolution governed by quark-gluon string model (QGSM) [12]. To check this, we have calculated the angular momentum at different points of time of the collision by taking into account the contributions from both the participants and spectators. We consider the Au + Au collisions with $b = 8$ fm at $\sqrt{s} = 5\,\mathrm{GeV/u}$, which is typical for the future Nuclotron-based Ion Collider fAcility (NICA) collider. We observe (see Fig. 1) that the participants carry about 10–20% of angular momentum and that the total angular momentum of participants and spectators is conserved within a good accuracy.

From this observation, one may conclude that the angular momentum is under good control in the QGSM model.

We also study correlations of angular momentum, participant fractions, and the hydrodynamic helicity and observe that these quantities vary in accordance with each other, provided that the helicity is defined in one of the hemispheres in accordance with the separation effect [5,8] discussed above. In order to perform this comparison and further calculations, velocity, vorticity, and helicity are determined following the earlier suggested procedure [5] where the respective quantities are properly averaged over events and particles within the three-dimensional cells providing the transition from the kinetic to hydrodynamic description.

In the following, we discuss the corresponding results.

Large-scale structures of vorticity fields. We start our studies with the qualitative structure of velocity and vorticity fields.

The general structure of velocity field follows the so-called little bang pattern, which may be quantified by the velocity dependence allowing one to extract the so-called little Hubble

*baznat@theor.jinr.ru
†gudima@theor.jinr.ru
‡sorin@theor.jinr.ru
§teryaev@theor.jinr.ru

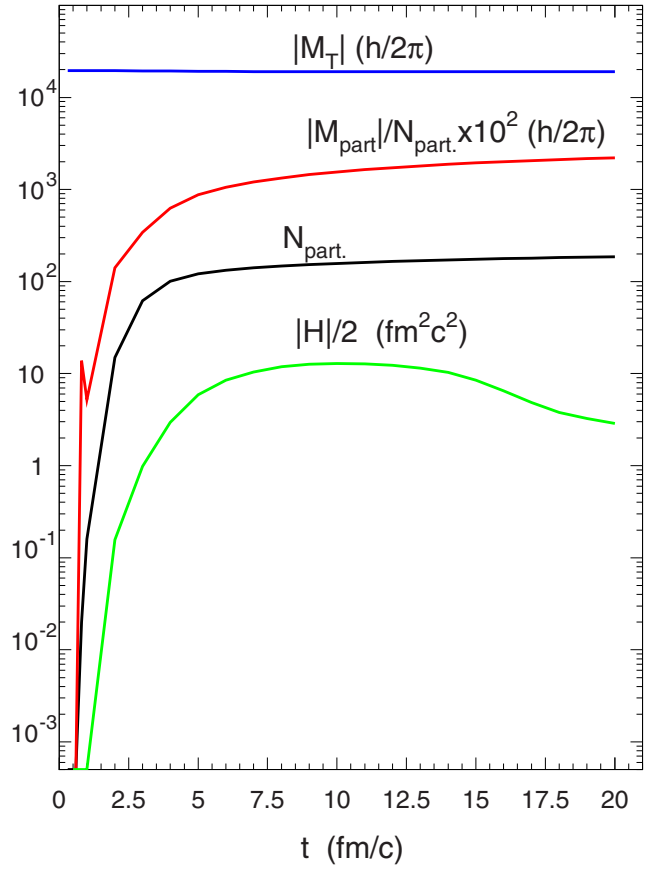

FIG. 1. The time dependence of the total (M_T) and participant (M_{part}) angular momenta in Planck constant units and that of participant amount (N_{part}) compared with hydrodynamical helicity (H).

constant. We calculate the dependence of average cell velocity on the transverse distance $\rho = \sqrt{x^2 + y^2}$ and find (see Fig. 2) that it is consistent with the linear Hubble law:

$$\langle v/c \rangle = v_0/c + H\rho. \tag{1}$$

The Hubble constant H is measured in the units of 10^{-22} s $=$ 30 fm/c and changes in the range

$$H = 0.024 \div 0.028\,(\text{fm/c})^{-1}.$$

It corresponds to the so-called little universe lifetime of about 40 fm/c, which is only twice larger than the collision time.

Our key observation is that while velocity field represents the little bang picture, vorticity field forms the relatively thin toroidal tirelike structures (Fig. 3). This emerges in the layer (where velocity field changes rapidly) separating the core and corona regions [13,14] and forms the sort of vortex sheet.

The interesting property of these structures is that, while emerging due to angular momentum pseudovector $\vec{M}$ in the noncentral collisions, they do not remember the production plane, and they possess the cylindrical symmetry with regard to (w.r.t.) collisions axis z. This may be observed (Fig. 4) by considering the vortex sheet in the case of the particular direction of $\vec{M}$ along the y axis.

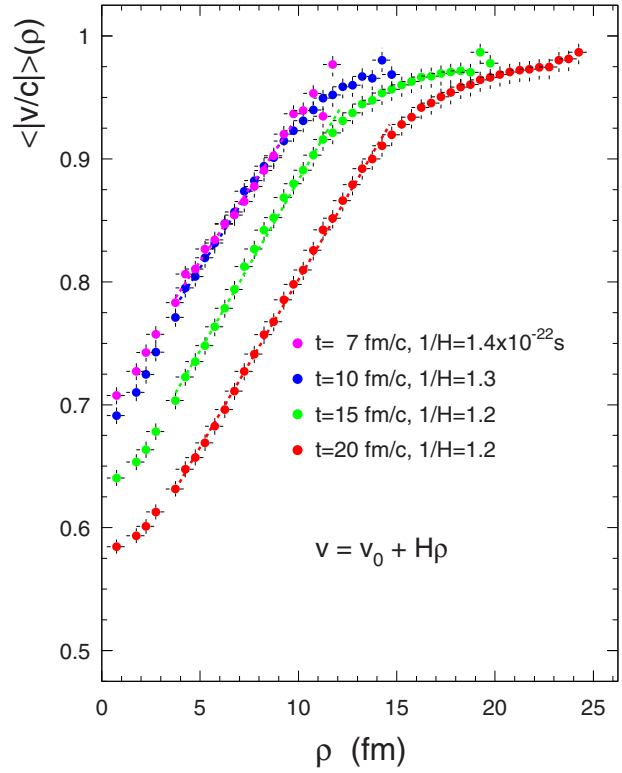

FIG. 2. The cell velocity dependence on the transverse distance.

Such behavior may resemble cyclones appearing at femtoscopic scale.

However, the feature that the vorticity field is significant at the surface contradicts the finding [10,15] based on UrQMD calculations. As described in Ref. [15], which deals with the experimental data on azimuthal Hanbury Brown and Twiss (HBT) correlations, one may think that our observation may depend on the specific model parameters, e.g., string tension.

This problem certainly deserves further investigation. However, the model with the same parameters that we use has also been tested [16] against experimental data on hypermatter production, which is actually a problem similar to the hyperon polarization we are going to study in the following.

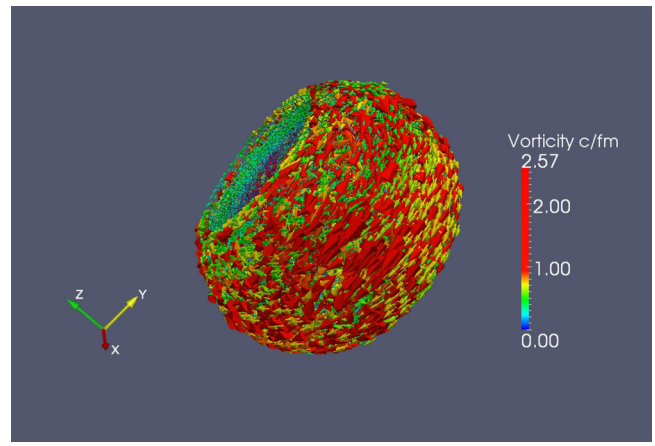

FIG. 3. The vortex sheet.

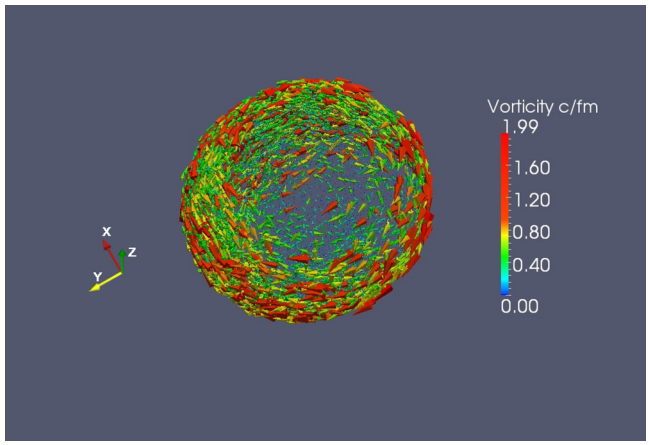

FIG. 4. The vortex sheet for the particular direction of angular momentum.

Hyperon polarization. We consider hyperon polarization as the observable related to vorticity and helicity [3]. We shall concentrate mostly on Λ hyperon production, which has some advantages: They are produced in large numbers, their polarization may be easily determined in their weak decays, and their spin is carried by strange quark.

As mentioned above, although Dubna Cascade Model (DCM)-QGSM model was already tested for description of the hyperon production at higher energies, we perform another test (see Fig. 5) comparing with the data [17] at 1.93 GeV, closer to NICA energy range. This is important as the polarization should be more pronounced at smaller energies where strange chemical potential is larger. The description of the data is quite satisfactory.

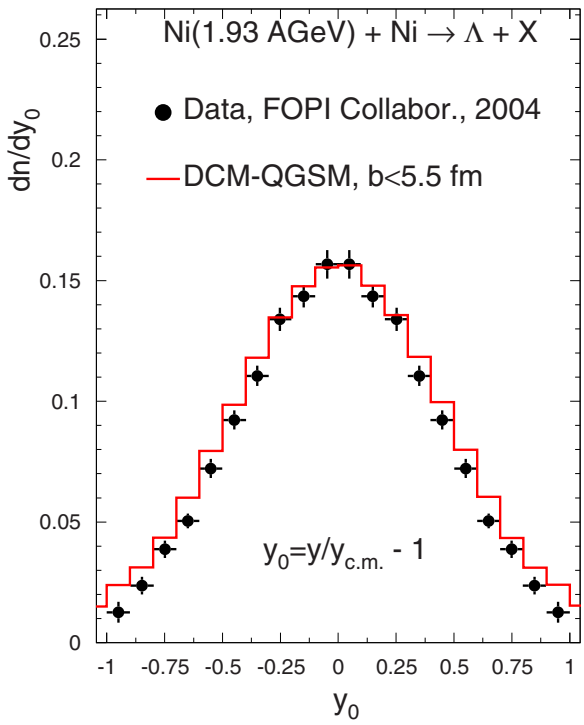

FIG. 5. Rapidity dependence of Λ hyperon multiplicity.

We compare the two rather distinct methods of determining the hyperon polarization. The first one corresponds to the earlier one suggested [3] and explored [5] in relation to the induced axial current while the second one follows the procedure based on the thermal vorticity [7].

The first method is based on the calculation of strange axial charge

$$Q_5^s = \frac{N_c}{2\pi^2}\int d^3x\mu^2(x)\gamma^2\epsilon^{ijk}u_i\partial_j u_k = \frac{\langle\mu^2\gamma^2\rangle\, N_c H}{2\pi^2}, \quad (2)$$

where $N_c = 3$ is the number of colors. The use of the (approximately) conserved charge is expected to make the result insensitive to the details of equilibration and formation of quark-gluon plasma. This may be compared to the relation of (axial) current correlators at quark and hadron levels due to quark-hadron duality (see, e.g., Ref. [18] and references therein).

In Ref. [5], we use the latter equality exploring the mean-value theorem. In this work, in addition, the spatial variation of strange chemical potential μ is taken into account. To do so, the description of kinetic distribution functions by the corresponding equilibrium equation is performed that provides the matching of kinetic and thermodynamical descriptions. As a result, the time dependence of the distribution of strange chemical potential takes the form represented at Fig. 6. Note that the vortex sheets are not directly seen here, contrary to Figs. 3 and 4. This may be related to the fact that vorticity is proportional to the velocity gradient, which is enhanced at the border between participants and spectators, which is, generally speaking not true for chemical potential. Let us also mention that the toroidal structure is absent (see Fig. 1 of Ref. [5]) for velocity itself. The average polarization can be

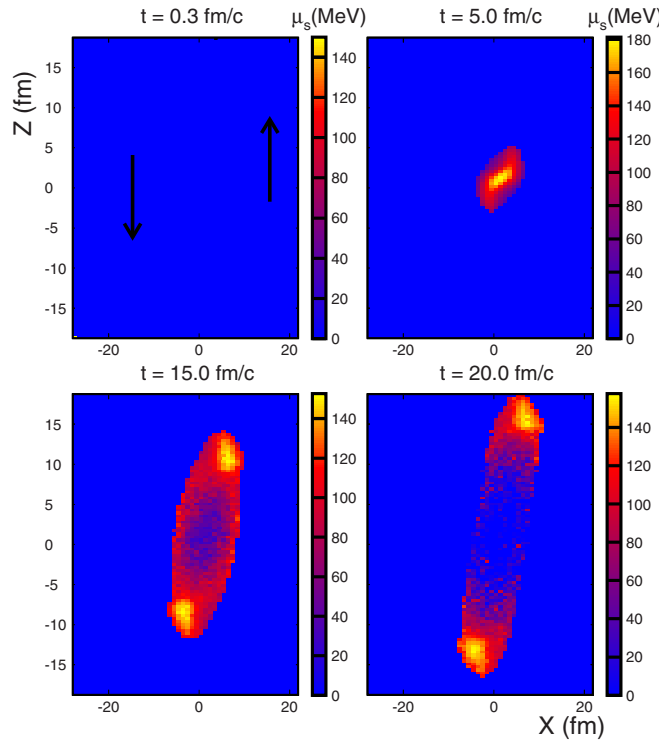

FIG. 6. The time dependence of strange chemical potential.

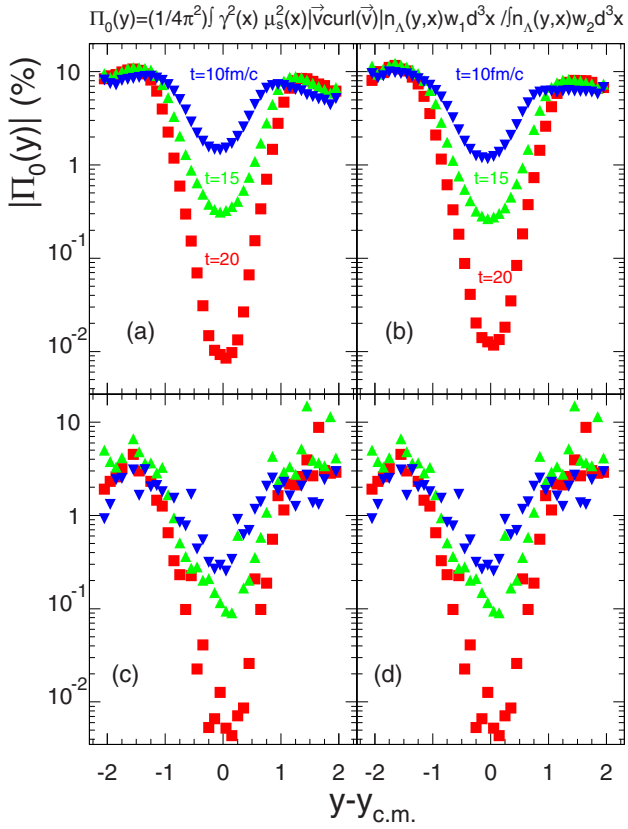

FIG. 7. The rapidity dependence of polarization in helicity-based approach.

estimated by dividing Q_5^s (2) by the number of Λ's, assuming that the pseudovector of axial current is proportional to the pseudovector of polarization, $Q_5^s \sim \langle \Pi_0^{\Lambda,lab} \rangle$. Selecting the axial charge related to the particles in the definite rapidity or transverse momentum interval, the respective dependence of polarization may also be obtained.

As the axial charge should be related to the zeroth component of hyperon polarization in laboratory frame Π_0^{lab}, the transformation to hyperon rest frame, where polarization is measured via the decay angular distribution, should be performed. Taking into account that the polarization pseudovector should be directed along the y axis (as it has to be collinear to $\vec{M}$ pseudovector), one gets

$$\Pi_0^{\Lambda,lab} = \frac{\Pi_0^{\Lambda}\, p_y}{M_\Lambda}, \tag{3}$$

where M_Λ is the hyperon mass. To get the (average) rest frame polarization, one should divide the axial charge by the number of hyperons n_Λ and obtain kinematical factor so that

$$\langle \Pi_0^{\Lambda} \rangle = Q_5^s \left\langle \frac{M_\Lambda}{n_\Lambda\, p_y} \right\rangle. \tag{4}$$

The preservation of positivity ($|\Pi_\Lambda| \geqslant 1$) or the absence of divergence is due to the fact that hyperons with zero y component of the momentum should not have the zeroth component of polarization, and therefore should not contribute to Q_5^s. To avoid this complication, one may instead attribute the factor p_y/M to each hyperon in the denominator of (4). We compare various ways of averaging of the kinematical boost factor (3). We include it in the either numerator of (4) or denominator. For completeness, we also include the (unphysical) calculations with the boost factor absent as well as with the factors appearing both in numerator and denominator and therefore squared. Please note that the two last ways of calculation are considered only to check the sensitivity of the result to the kinematical boost factor. Nevertheless, the comparison (see Fig. 7) of various approaches shows the similar scale and rapidity dependence of polarization.

Another approach to polarization is based on the so-called thermal vorticity [7]. To provide the comparison, we calculate (see Fig. 8) the thermal vorticity field and the respective polarization.

While a scale of the polarization in the thermal vorticity-based approach is several times larger, its rapidity dependencies surprisingly appear to be similar in these rather distinct approaches. Let us stress that such similarity is due to the fact that thermal vorticity is calculated in the kinetic DCM-QGSM model. In the case of hydrodynamic model, e.g., in the original work in Ref. [7], the rapidity dependence is different due to the large transparency of our model and late formation of hyperons.

One may relate the growth of polarization in the fragmentation regions to the already discussed appearance of the tirelike structure where vorticity and helicity are enhanced. The particles from these regions should have more opportunities

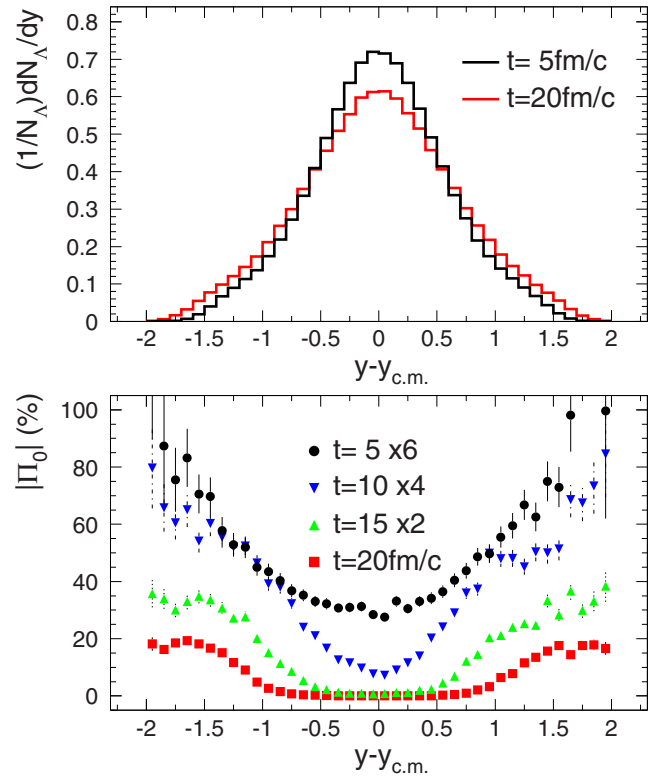

FIG. 8. The rapidity dependence of the multiplicity and polarization in the thermal vorticity-based approach. The magnitudes of polarization at different times are rescaled by the identified factors.

to fly in forward (backward) directions in the center-of-mass (c.m.) frame. This is absent in the hydrodynamical models. Therefore, the growth of polarization in the fragmentation region may be considered as an indirect probe of such a structure formation.

Conclusions and outlook. We have investigated vorticity and hydrodynamical helicity in noncentral heavy-ion collisions in the framework of the kinetic quark-gluon string model. We have confirmed our earlier observation that the vorticity field is predominantly localized in a relatively thin layer ($2 \div 3$ fm) on the boundary between the participant and spectator nucleons and observed that it forms the specific toroidal structures, which may be considered as vortex sheets with the unexpected cylindrical symmetry. They look like cyclones appearing at femtoscopic scale. The comparison with other approaches where these structures do not appear requires further investigation.

The vorticity and helicity fields are manifested in the Λ hyperon polarization. We have performed its detailed calculations including the simulations of the strange chemical potential. We have found that the polarization magnitude may reach a percent level. The comparison with distinctly different approach exploring the thermal vorticity leads to qualitatively similar results, although the polarization scale is several times larger. The growth of polarization in the fragmentation regions may be considered as an indirect probe of toroidal structures formation.

Acknowledgment. This work was supported in part by the Russian Foundation for Basic Research, Grant No. 14-01-00647.

[1] K. Fukushima, D. E. Kharzeev, and H. J. Warringa, The Chiral Magnetic Effect, Phys. Rev. D **78**, 074033 (2008).

[2] D. Kharzeev and A. Zhitnitsky, Charge separation induced by P-odd bubbles in QCD matter, Nucl. Phys. A **797**, 67 (2007).

[3] O. V. Rogachevsky, A. S. Sorin, and O. V. Teryaev, Chiral vortaic effect and neutron asymmetries in heavy-ion collisions, Phys. Rev. C **82**, 054910 (2010).

[4] T. Kalaydzhyan, Temperature dependence of the chiral vortical effects, Phys. Rev. D **89**, 105012 (2014).

[5] M. Baznat, K. Gudima, A. Sorin, and O. Teryaev, Helicity separation in heavy-ion collisions, Phys. Rev. C **88**, 061901 (2013).

[6] J.-H. Gao, Z.-T. Liang, S. Pu, Q. Wang, and X.-N. Wang, Chiral Anomaly and Local Polarization Effect from Quantum Kinetic Approach, Phys. Rev. Lett. **109**, 232301 (2012).

[7] F. Becattini, L. P. Csernai, and D. J. Wang, Λ polarization in peripheral heavy ion collisions, Phys. Rev. C **88**, 034905 (2013).

[8] O. Teryaev and R. Usubov, Vorticity and hydrodynamic helicity in heavy-ion collisions in the hadron-string dynamics model, Phys. Rev. C **92**, 014906 (2015).

[9] L. P. Csernai, V. K. Magas, and D. J. Wang, Flow vorticity in peripheral high energy heavy ion collisions, Phys. Rev. C **87**, 034906 (2013).

[10] V. Vovchenko, D. Anchishkin, and L. P. Csernai, Time dependence of partition into spectators and participants in relativistic heavy-ion collisions, Phys. Rev. C **90**, 044907 (2014).

[11] L. P. Csernai, D. J. Wang, M. Bleicher, and H. Stocker, Vorticity in peripheral collisions at the Facility for Antiproton and Ion Research and at the JINR Nuclotron-based Ion Collider Facility, Phys. Rev. C **90**, 021904 (2014).

[12] V. D. Toneev, N. S. Amelin, K. K. Gudima, and S. Y. Sivoklokov, Dynamics of relativistic heavy ion collisions, Nucl. Phys. A **519**, 463c (1990); N. S. Amelin, K. K. Gudima, S. Y. Sivoklokov, and V. D. Toneev, Yad. Fiz. **52**, 272 (1990) [Sov. J. Nucl. Phys. **52**, 172 (1990)]; N. S. Amelin, E. F. Staubo, L. P. Csernai, V. D. Toneev, and K. K. Gudima, Strangeness production in proton and heavy ion collisions at 14.6-A/GeV, Phys. Rev. C **44**, 1541 (1991).

[13] J. Aichelin and K. Werner, Centrality dependence of strangeness enhancement in ultrarelativistic heavy ion collisions: A core-corona effect, Phys. Rev. C **79**, 064907 (2009); **81**, 029902(E) (2010).

[14] J. Steinheimer and M. Bleicher, Core-corona separation in the UrQMD hybrid model, Phys. Rev. C **84**, 024905 (2011).

[15] G. Graef, M. Bleicher, and M. Lisa, Twisted emission geometry in noncentral Pb + Pb collisions measurable via azimuthally sensitive Hanbury-Brown-Twiss correlations, Phys. Rev. C **89**, 014903 (2014).

[16] A. S. Botvina, K. K. Gudima, J. Steinheimer, M. Bleicher, and I. N. Mishustin, Production of spectator hypermatter in relativistic heavy-ion collisions, Phys. Rev. C **84**, 064904 (2011).

[17] X. Lopez (FOPI Collaboration), Results from FOPI on Λ production in Ni + Ni collisions at 1.93-A-GeV, Prog. Part. Nucl. Phys. **53**, 149 (2004).

[18] Y. N. Klopot, A. G. Oganesian, and O. V. Teryaev, Axial anomaly as a collective effect of meson spectrum, Phys. Lett. B **695**, 130 (2011).